

Title: The interaction between Lateral size effect and Grain size when scratching polycrystalline copper using a Berkovich indenter

A. KAREER^{1,2}, X. D. HOU³, N. M. JENNETT⁴ and S. V. HAINSWORTH²

1. Department of Materials, University of Oxford, Parks Road, Oxford, OX1 3PH
2. Department of Engineering, University of Leicester, University Road, Leicester, LE1 7RH, UK
3. Materials Division, National Physical Laboratory, Teddington Middlesex TW11 0LW, UK
4. Faculty of Engineering, Environment and Computing, Coventry University, Coventry, UK

Abstract

It has been reported previously that, for single and polycrystalline copper (fcc), the indentation size effect (ISE) and the grain size effect (GSE) can be combined in a single length-scale-dependent deformation mechanism linked to a characteristic length-scale calculable by a dislocation-slip-distance approach (Hou et al, Acta. Mater. 2012). Recently, we identified a “lateral size effect (LSE)” in scratch hardness measurements in single crystal copper, where the scratch hardness increases when the scratch size is reduced (Kareer et al., Philos. Mag. 2016).

This paper investigates the effect of grain size on the scratch hardness of polycrystalline copper with average grain sizes between 1.2 μm and 44.4 μm , when using a Berkovich indenter. Exactly the same samples are used as in the indentation investigation by Hou et al. (Acta Mater. 2012). It is shown that, not only does the scratch hardness increase with decreasing grain size, but that the GSE and LSE combine in reciprocal length (as found previously for indentation) rather than as a superposition of individual stresses. Applying the same (as indentation) dislocation-slip-distance-based size effect model to scratch hardness yielded a good fit to the experimental data, strongly indicating that it is the slip-distance-like combined length-scale that determines scratch hardness. A comparison of the fit parameters obtained by indentation and scratch on the same samples is made and some distinct differences are identified. The most striking difference is that scratch hardness is over four times more sensitive to grain size than is indentation hardness.

1. Introduction

The scratch test has become widely popular for characterising the adhesive and fracture properties of thin films and coatings [1]–[6] and is also used to investigate small scale wear phenomenon, such as automotive and optical applications [7]–[9]. Very often the scratch test is only able to return quasi-quantitative measurements, e.g. critical load value (L_c) for a particular coating failure in a ramped load test. The instrumented indentation community has increasingly sought to interpret hardness tests and indentation response as being a function of

the constitutive properties of the indented materials [10, 11] with indentation stress-strain curves being one example of this [see ISO\TR 29381 for a summary of methods]. This research has resulted in the identification and quantification of indentation size effects linked to the variation of dislocation generation and mobility in a material, as a function of the materials microstructural length scale and indentation plastic zone size etc. Indentation size effects have been observed for a range of metals, where the indentation hardness (at a constant indentation strain) increases as the indents get smaller [12]–[14]. In addition, the Hall-Petch grain size effect [15] [16] has been observed, in samples of copper, to interact with indentation size such that indentation hardness increases with the reciprocal sum of the individual length scales of indent size and grain size [17][18]. Hardness is also affected by dislocation density, for example Taylor Forrest hardening [19]; and work hardening, as the name implies, is the well-known increase in hardness with increasing plastic strain (cold work). The specific dislocation density and plastic zone size generated by indentation is a function of the indenter geometry and the indentation strain applied [20]. Hou et al. performed indentation with both spherical and Berkovich indenters on samples of pure copper with a range of grain sizes [18] and showed that dislocation density interacts with grain size and indent size to affect hardness results and that this can be described as the formation of an average spacing between obstacles (to dislocation motion), where this spacing can be directly related to indentation hardness; they found that all hardness data could be fitted by a single mathematical function:

$$H = H_0 + \left(\frac{k_1}{a} + \frac{k_2}{d} + k_3 \sqrt{\rho_s} \right)^{0.5} \quad \text{Equation 1}$$

Where H is the indentation hardness, H_0 is the size-independent hardness, a is the contact radius of the indentation, d is the average grain size of the material, ρ_s is the dislocation density and k_{1-3} are scaling parameters to adjust the input lengths to the actual (but not so measurable) lengths that are constraining dislocation generation and motion. Hou et al. have shown that hardness is, therefore, rapidly dominated by the smallest length-scale and, in practice, the interaction between length-scales is only apparent when they are within a factor of 6-10 of each other. E.g. varying the size of a large indent has no significant effect if some other length-scale (e.g. grain size or dislocation spacing) is more than a factor of 6 to 10 smaller.

Indentation hardness is often the parameter of choice to predict tribological performance. However, many surface damage mechanisms occur in direct shear, where a ‘scratching’ action is a more direct representation of the failure event. Therefore, scratch testing is a much closer simulator or predictor of tribological performance. It is ironic that the original concept of hardness was based on the ability of one material to scratch another [21]. With many designers wishing to enhance the properties of components by the introduction of nano-scale materials, and test their properties, it is increasingly important to identify whether the same size effects

that are observed in indentation, are applicable and active when scratching. It is, similarly, essential that any plasticity theory or analysis used, is able to predict both types of event. The modified slip-distance theory is an excellent predictor of indentation hardness response in polycrystalline copper and therefore is an obvious candidate theory to adopt, in order to understand the scratch hardness response.

Scratch hardness tests on the macroscopic scale exist, e.g. the ASTM G171 standard, where constant normal force scratches are produced using a spherical indenter (Rockwell C geometry); the calculation of scratch hardness uses the normal force applied, divided by the projected area of contact, which is defined as a semicircle with a diameter equivalent to that of the scratch width [22]. Typical scratch widths are of the order of hundreds of microns and easily measurable using direct optical imaging; the normal forces applied are larger than 1N. However, in order to investigate the surface properties of nano and micro-structured materials and the plasticity size effects at operating at those scales, is it essential to reduce the scale of the test. The advent of advanced instrumented indentation testing (IIT) systems has allowed nano-scale scratch experiments to be performed using ultra low loads and displacements on the order of nanometers with a high level of control and measurement accuracy. Optically encoded and/or Piezo driven stages provide the capability for precise lateral motion, beneath a loaded indenter, to generate micro- or nano-scale scratches. Typical scratch depths of 50 nm – 1 μ m and forces in the region of 0.5 mN – 100 mN, are now routine and the techniques established in IIT allow accurate and precise measurement of scratch size, which is not possible using traditional optical imaging techniques.

Scratch testing is a conceptually simple test that, in reality, generates a complex and dynamic elastic and plastic response: a contact, with a contact area that is difficult to define, slides parallel to the surface whilst being acted upon by both a normal and a lateral force. Defining a scratch hardness that has a physical meaning is therefore challenging. Nevertheless, a method to determine the scratch hardness of single crystal copper using the Berkovich indenter geometry has recently been developed [23]. This goes beyond previous, simplified analysis approaches (of normal force divided by estimated contact area) and takes a more genuinely multiaxial approach; showing that it is necessary to incorporate both the normal and lateral forces acting on the indenter into the scratch hardness calculation, as both these forces individually contribute to the scratch response. Use of a Berkovich indenter allows the direction of the resolved force (normal and lateral) to be determined from the angle of the facet it is acting on. It is also more reasonable to assume that the force is uniformly distributed over the indenter facet(s), which is not the case for a sphero-conical indenter. Using a pre-calibrated area function of the indenter, the area of contact can be determined from the scratch penetration depth and

the fact that either one or two thirds of the total contact area is used, depending on whether the indenter is scratching face forward or edge forward.

In a previous paper [23] we found that, for single crystal copper, scratch hardness displayed a lateral size effect (LSE). Scratch hardness was calculated in three different ways and, in all cases, the nano/micro-scale scratch hardness increased with decreasing scratch size in a manner comparable to the indentation size effect (ISE). Since most technologically useful materials are polycrystalline, and instrumented indentation shows an interaction between indentation size and grain size, this paper is a first attempt to investigate the effect of grain size on the lateral size effect. To this end, the exact same samples used by Hou et al [18] were used in this study, in order to provide a direct comparison of the indentation size effect vs. the lateral size effect when combined with the grain size effect.

2. Method

A sample of (1 0 0) single crystal copper (Goodfellow Ltd, Cambridge, UK) and electroformed samples of polycrystalline copper (obtained from National Physical Laboratories (NPL), Teddington UK) were used for this study; preparation details for the polycrystalline samples are provided in [17] and the exact same specimens were used as in [18]. The single crystal was annealed for 4 hours at 200°C to reduce the dislocation density. All specimens were mechanically polished, followed by an electro-polish, to obtain a flat surface with minimum residual stress. An FEI Sirion scanning electron microscope (SEM) with a field emission gun (FEG) and an HKL Nordlys EBSD detector was used to obtain grain orientation maps by Electron Backscatter Diffraction (EBSD), to which the line intercept method was applied to obtain the average grain size of each sample as shown in Figure 1.

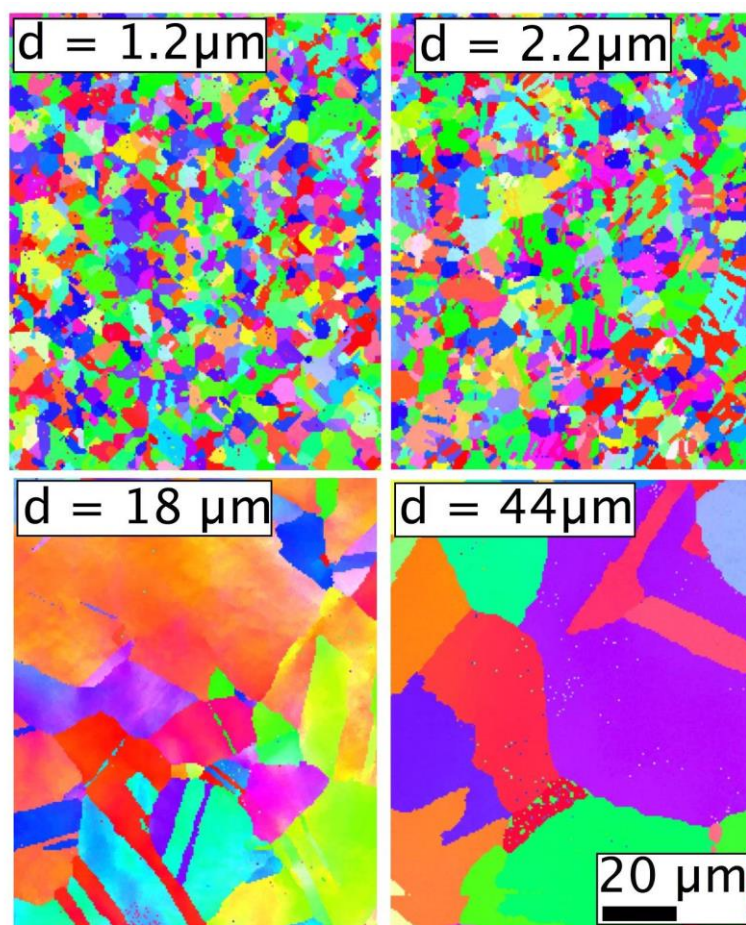


Figure 1 - EBSD maps of the polycrystalline samples, indicating the average grain size obtained from the line intercept method.

Scratch experiments were performed using an Agilent G200™ instrumented indentation system fitted with a lateral force measurement (LFM) probe and using a Berkovich indenter, oriented in the Edge forward (EF) position. Prior to any scratches being made, direct measurement of the indenter tip shape was performed at NPL, using a metrological atomic force microscope (AFM) (Park Autoprobe M5, Veeco instruments, Pasadena CA) to derive an area function for the contact area of the tip as a function of distance from the apex. A ‘three-pass’ (profile/scratch/profile) method was used with a constant scratch force. The first pass performed a profile of the surface topography using a normal force of 20 μN , over a distance of 140 μm . The second pass was the scratch segment; the first 20 μm of the segment was performed at the profiling force (20 μN) at which point the lateral movement of the tip was held stationary and the normal force was increased to the scratch force. This force was kept constant for a distance of 100 μm (the scratch length) after which the load was reduced again to the profiling force, for the remaining 20 μm . The final pass of the experiment performed a profile of the residual scratch track with a normal force of 20 μN for the entire 140 μm scratch distance. Figure 2 gives a typical scratch profile.

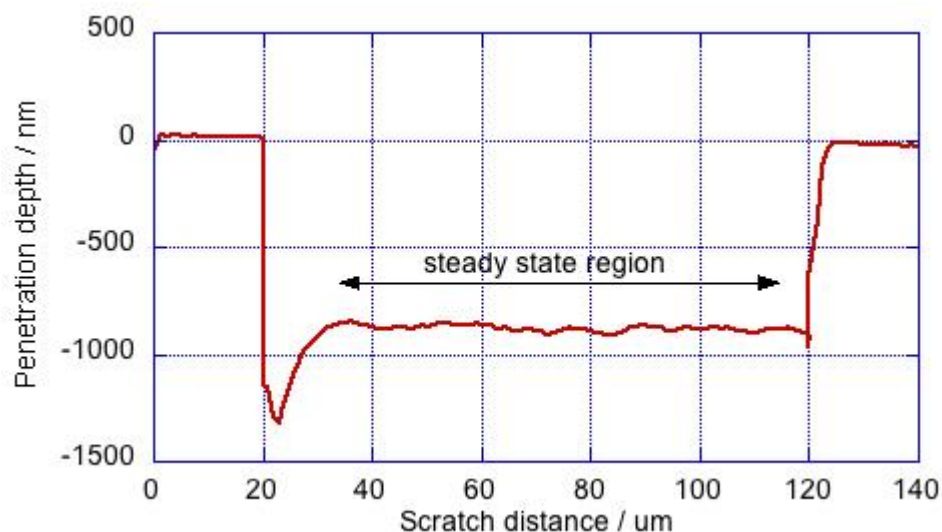


Figure 2 – Typical scratch penetration depth after correction for topography (taken from the corrected penetration depth channel) as a function of scratch distance.

All scratches were performed at a velocity of 10 $\mu\text{m}/\text{sec}$ in the EF tip orientation; the normal force ranged from 0.5 mN – 40 mN. For each normal force, 5 repeat experiments were performed. Output channels from the G200 system included the normal force, the lateral force, the indenter displacement and the corrected penetration depth. The corrected penetration depth is the real-time subtraction of the original topography scan from the scratch segment and corrects for surface tilt and roughness to give the penetration depth at any point. All output data was recorded as a function of scratch distance.

2.1 Calculation of scratch hardness

Single values of normal force, lateral force and penetration depth were obtained by averaging all values over the steady state region of the scratch (i.e. for each channel, an average of all values obtained between 35 μm and 115 μm shown in Figure 2). The contact surface area was taken to be two thirds of the total indenter surface area at the averaged penetration depth (two facets in contact for an edge forward scratch). Scratch hardness was calculated by resolving the average normal and average lateral force with respect to the tip orientation (see appendix) and dividing by the surface area in contact. A full description of the scratch hardness calculation is provided in [23]. Note that the contact area taken at the average penetration depth is an underestimate of the actual area of contact, because pile up above the original surface plane occurs. Direct measurements of the pile-up height (and scratch width, L) of scratches, in a single crystal copper sample, were obtained by AFM. Figure 3 is a plot of pile-up height normalised to the remnant depth below surface vs. scratch width, L . This shows that the normalised pile up height is constant with scratch width, approximately 1.6, and that the average penetration depth is proportional to scratch width, L . Thus the easier to measure parameter, average penetration

depth, is directly proportional to ‘scratch size’ and has therefore been used as a proxy parameter throughout this work.

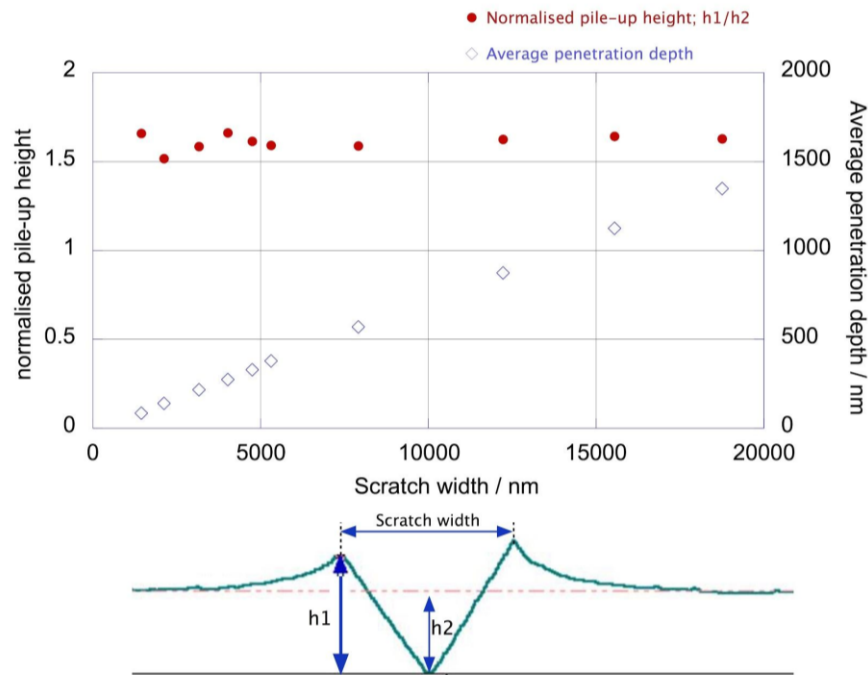


Figure 3 – Plots of measurements obtained by AFM showing: (RHS scale) Normalised pile-up height vs. scratch width for scratches performed on a sample of single crystal copper, (LHS scale) The average penetration depth vs. scratch width (L).

2.2 Analysis method

The analysis method in [18] uses Equation 1 to combine three critical length-scales (indentation size, grain size and dislocation density) in order to predict the indentation hardness. The variables in Equation 1 can be adapted in order to predict the scratch hardness values obtained, in a similar manner (i.e. by combining the three contributing length-scales) as follows:

$$H_s = H_0 + \left(\frac{k_1}{h} + \frac{k_2}{d} + k_3 \sqrt{\rho_s} \right)^{0.5} \quad \text{Equation 2}$$

Where H_s is the scratch hardness and h is the average penetration depth. All other variables remain the same as indicated in Equation 1. Values for the scaling coefficient k_1 were obtained from the gradient of a linear fit to $(H_s - H_0)^2$ vs. $1/h$ for each sample; the intercept of the fits provide a value of the $k_3 \sqrt{\rho_s}$ term in the case of the single crystal, and a value of $(k_2/d + k_3 \sqrt{\rho_s})$ in the polycrystalline samples. Using the obtained values of k_1 , a linear fit to a plot of $[(H_s - H_0)^2 - k_1/h]$ vs. $1/d$, yields a gradient of k_2 and an intercept of $k_3 \sqrt{\rho_s}$. Subtracting k_2/d from the $(k_2/d + k_3 \sqrt{\rho_s})$ values obtained from the original fits yields values of $k_3 \sqrt{\rho_s}$ individual to each polycrystalline sample.

3. Results

3.1 Scratch hardness results

Scratch hardness, determined using the method outlined above and in [23], are plotted against the average penetration depth in Figure 4. Two size effects are observed; a lateral size effect where the scratch hardness increases with decreasing average penetration depth, and a grain size effect where the scratch hardness increases with decreasing grain size. Both size effects combine in each scratch. In order to investigate the grain size effect, scratch hardness values of scratches with approximately the same penetration depth are compared in Table 1, alongside the measured normal and lateral forces.

Figure 5 shows the scratch hardness plotted against the inverse square root of the grain size. Each data point represents the average of 5 scratches at a particular normal force. The extent of the lateral size effect for each sample is given by the vertical spread of the data. The LSE ratio is also shown in Figure 5. This ratio is the highest scratch hardness obtained on a sample divided by the lowest scratch hardness on that sample.

Since the scratch results in this paper were obtained from the exact same samples as the indentation results in [18], it is possible to make a direct comparison of the scaling coefficients, k_i , obtained by indentation and by scratch testing. Table 2 shows the values obtained for the scaling coefficients in Equation 2 as a function of grain size.

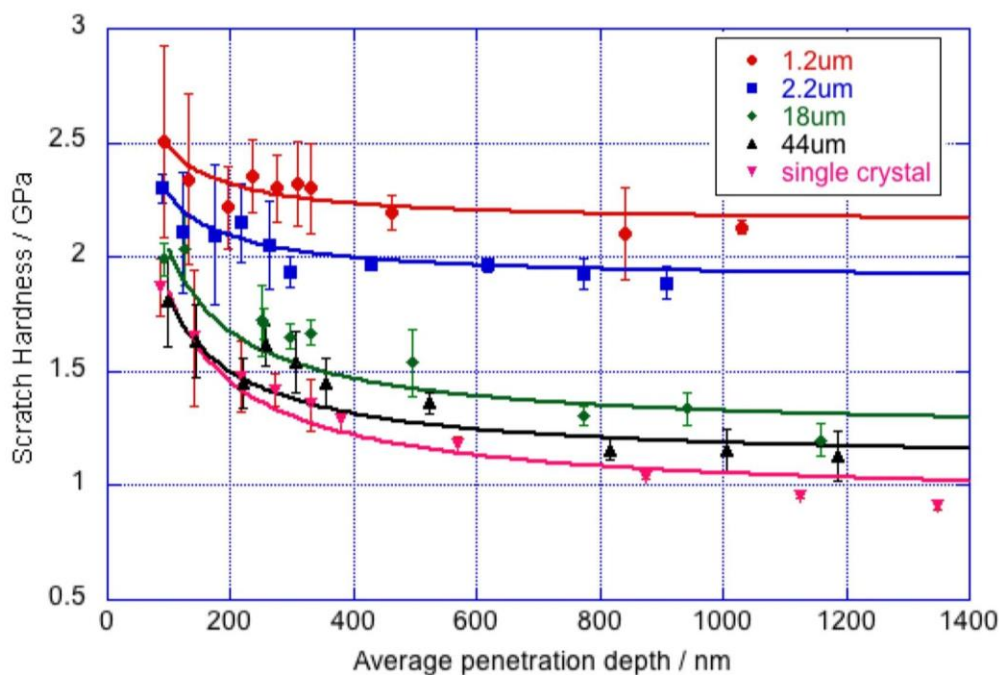


Figure 4 – Scratch hardness of polycrystalline copper plotted against the average penetration depth, for all specimens: $d=1.2\mu\text{m}$ (closed triangles), $d=2.2\mu\text{m}$ (open squares), $d=18\mu\text{m}$ (open circles) and $d=44\mu\text{m}$ (closed diamonds). Each data point represents the average of 5

measurements at a particular normal force; error bars represent one standard deviation. Solid lines show the simulated scratch hardness from Equation 2 using the scaling coefficients provided in Table 2; $H_0 = 0.045$ GPa.

Table 1 - Comparison of lateral force values vs. grain size for same-sized scratches.

Grain size / μm	Average penetration depth / μm	Normal Force / mN	Lateral Force / mN	Scratch Hardness / GPa
1.2 ± 1	0.89 ± 0.01	30 ± 0.03	20 ± 0.07	2.3 ± 0.02
2.2 ± 0.8	0.88 ± 0.27	40 ± 0.09	20 ± 0.21	2.0 ± 0.07
18 ± 15	0.90 ± 0.28	30 ± 0.04	14 ± 0.42	1.3 ± 0.07
44 ± 25	0.84 ± 0.52	20 ± 0.04	10 ± 0.34	1.2 ± 0.05
Single Crystal	0.87 ± 0.15	20 ± 0.05	7.5 ± 0.14	1.0 ± 0.01

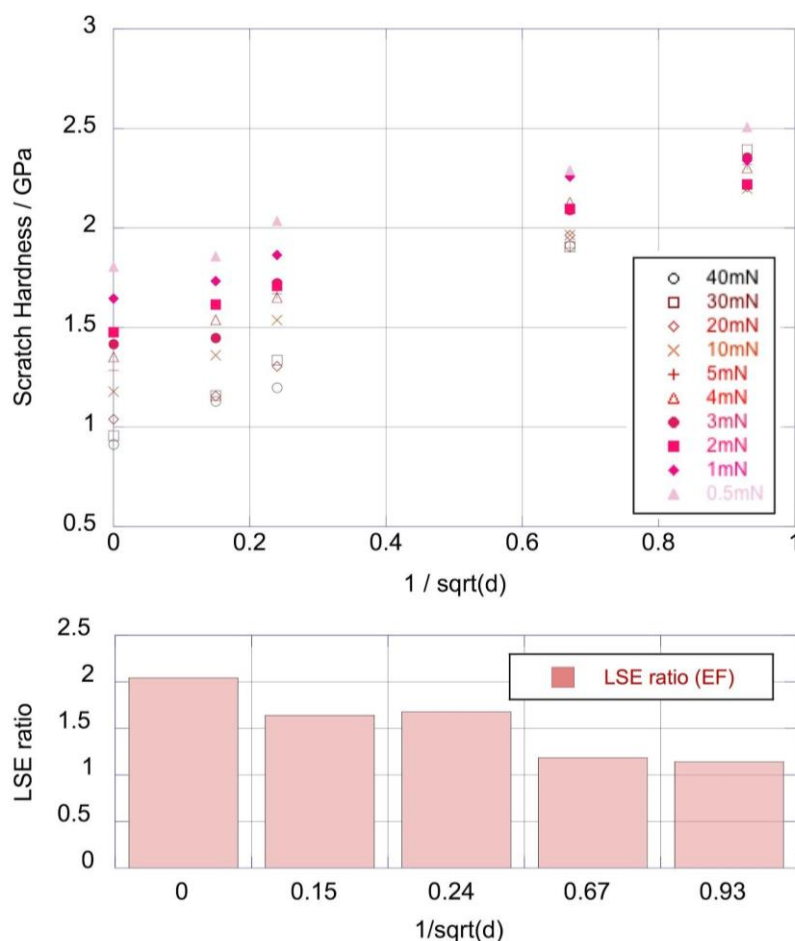


Figure 5– Scratch hardness of all scratch sizes, on all samples, including the single crystal, plotted as a function of $1/\sqrt{d}$. Each data point represents the average of 5 scratches performed at a particular normal force (0.5mN–40mN). Error bars are not included. Scratch hardness increases with decreasing normal force, hence the lateral size effect is observed in the vertical spread of the data.

Table 2 - Comparison between Indentation size effect (ISE) and lateral size effect (LSE) values for individual size effect scaling coefficients / [$\text{m}\cdot\text{GPa}^2$]. Values for ISE are taken from [18]; $H_0 = 0.045 \text{ GPa}$.

Grain size / μm	LSE			ISE		
	k_1	k_2	$k_3\sqrt{\rho_s}$	k_1	k_2	$k_3\sqrt{\rho_s}$
1.2 ± 1	0.16	3.48	1.6	1.1	0.85	0.24
2.2 ± 0.8	0.058		2.0	0.71		0.26
18 ± 15	0.26		1.3	-		-
44 ± 25	0.21		1.1	-		-
Single Crystal	0.25	($d = \infty$)	0.9	1.6	($d = \infty$)	0.22

4. Discussion

A plot of the scratch hardness data for each sample is given in Figure 4, together with the fits obtained by using Equation 2. It can be seen that Equation 2 is a very good fit to the scratch data, passing within 1 standard deviation of most data points, and with the trends in the scratch data also followed well by the fit. The data itself shows a clear Lateral Size Effect (LSE), where, for every sample, smaller scratches are harder. In addition, there is a clear grain size effect, with smaller-grained samples being systematically harder. The interaction between LSE and grain size is shown more clearly in Figure 5. Here, the results from scratches using the same range of applied scratch forces are plotted for each sample of different grain size; the lateral size effect can be seen as the range of scratch hardness values for each sample. There is a clear decrease in LSE as the grain size decreases. This has been specifically expressed at the bottom of Figure 5, where the LSE ratio (the scratch hardness value from the smallest (hardest) scratch divided by the value for the largest (softest) scratch) are plotted for each sample. The observed reduction in LSE ratio with reduction in grain size is similar to the reduction in ISE ratio vs. grain size observed for indentation in [17, 18]. It is therefore evident that, in both indentation and scratch, the two length-scales of test size and grain size are combining rather than generating independent additional stress contributions that then superpose. The slip-distance-like combination of length-scales in Equation 2 is, therefore, able to explain not only the individual

effects of test size and grain size, but also the way that these two length-scales interact to generate a material response.

Accepting that equation 2 is able to describe and predict scratch test response, the fit values of the scaling parameters can now be inspected to derive further physical insight. Table 2 lists the values of the scaling factors, k_{1-3} , obtained from the fits to the data for each sample. The necessity (and utility) of these scaling factors is to convert the input length-scales (e.g. indent size, a , grain size, d , etc.) into the actual (but not as easily measured) length-scales of importance to dislocations (i.e. h/k_1 , d/k_2 etc.). For example, this enables the analysis automatically to take into account unknown factors, such as values of Schmid factor for the actual slip planes activated. When a scaling factor is smaller than 1, this means that the measured length used is underestimating the real length-scale of interest. It can be seen from Table 2 that the scratch test value for k_1 is less than 1, which implies that the test-induced plastic zone size is, in fact, larger than the input length (scratch depth) used to represent it. Similarly; the scratch test k_2 value in Table 2 is 3.48 times bigger than unity, which implies that the effective grain size experienced by the dislocations/sources is much smaller than the input measured length (grain size). Given that the measurement of dislocation density and/ or spacing is notoriously difficult, a quantitative value of $k_3\sqrt{\rho_s}$ offers the possibility of indirect quantification of these values and, therefore, quantification of concepts such as “work hardened state” which are currently semi-quantitative at best.

Given that the length-scale-based analysis has been successfully applied to both indentation and scratch test data, obtained from exactly the same samples as used by Hou et al [17] [18], it is natural to compare the absolute values of the fit parameters obtained for indentation and scratch testing. It can be seen that the values obtained for the k_i values are considerably different. This is to be expected where, for convenience, different (but geometrically proportional) input parameters have been used, but could also occur is different-length scales of interest (i.e. determine) the deformation in each test. The LSE k_1 values for the single crystal and 1.2 μm grain size materials are about 6.4 and 6.8 times less than the k_1 values for ISE respectively. The 2.2 μm grain size sample has an anomalously large ISE/LSE k_1 ratio of over 12. Considering first the geometrical equivalence of the input parameters chosen. The LSE to ISE difference can be partly explained by the fact that LSE values obtained using the different proxy parameter of average penetration depth. This was the easiest parameter to obtain from the scratch test data as it is a direct output in the scratch dataset and can be obtained without any further imaging or external characterisation equipment. Scratch depth (average penetration depth) is, however, a completely different geometric parameter of average penetration depth does not include pile-up. Once pile-up is taken into account (see Figure 3), the actual penetration depth is approximately 1.7 times the average penetration depth. There is then a further geometric

correction to be made for the use of penetration depth in the scratch analysis instead of contact radius. For a perfect Berkovich indenter the actual penetration depth is approximately 2.8 times less than the contact radius. Thus, taking both corrections together, the values of k_1 for LSE (based on average penetration depth) might be expected to be $1.7 \times 2.8 = 4.8$ times less than those for indentation. However, even after making these corrections there remains a difference in ISE/LSE k_1 ratio of 1.3-1.4 for single crystal and 1.2 μm grain size respectively, or 4.3 for the 2.2 μm grain size sample. It is clear that this slip-distance-based analysis is directly indicating that scratching generates a larger plastic zone than in a similar sized indentation and that selection of a scratch dimension equivalent to the length scale used in indentation testing is not appropriate to characterise the deformation occurring in the scratch test.

This lack of direct equivalence of critical deformation length-scale is perhaps not surprising, a more traditionally selected dimension is the scratch width, L , which is, in this case, exactly the side length of the indenter and is the projected lateral size of the indenter travelling sideways. If you consider a scratch to be a sideways indentation, where $L/2$ is equivalent to a , then, by geometry at any depth, h , $L/2$ is equal to $1.35a$ for a perfect pyramid. Interestingly, if this is the case, then LSE and ISE k_1 values are in very good agreement.

The most striking result obtained is that the grain size effect in scratch hardness is significantly different to that observed in indentation testing. It can be seen, from Table 2, that the LSE k_2 is over four times larger than ISE k_2 , despite the fact that the grain size values used are the same in both analyses and exactly the same samples were tested. More specifically, the fit to the scratch test data shows that the scratch test behaves as if the effective microstructural length scale is 3.48 times less than the average grain size. In contrast an indentation responds as is the effective microstructural length scale is much closer to the grain size. Some useful insight into the deformation processes around a scratch stylus was recently obtained by Li and Szułfarska [25] who used LAMMPS molecular dynamics software [26] to simulate spherical and cylindrical-flat-punch tips scratching polycrystalline copper. These simulations predict that a laterally travelling stylus continuously generates/regenerates a well-defined zone of plasticity ahead of itself, in which new grain boundaries are formed, by concentration and rearrangement of dislocations, to provide a plane of easy slip. This suggests that, local to the stylus, the grain size could well be less than that of the undisturbed material, which is consistent with our analysis of scratch hardness.

Another consideration is that there are significant differences between the actual grain sizes interacting with the indentation plastic zone size vs. the scratch test plastic zone. An indentation plastic zone extends statically into a material grain structure. It is therefore mostly below the surface and interacting with entire grains in all directions of the half-space indented. Scratch testing however, generates more surface plasticity and the plastic zone is travelling dynamically

through the material surface region, interacting with the quarter-space in the forward direction. The surface is more likely to contain fractional grains (particularly on a well-polished surface) and the plastic zone will be interacting only with the grains in front of the stylus.

The effects of uncertainties in the determination of k_2 are also worth considering. Equation 2 requires an input of the size-independent hardness, H_0 . In [18], H_0 was taken to be three times the yield stress (15 MPa) obtained from an uniaxial compression testing of $\sim 100 \mu\text{m}$ grain size high purity copper [14]. This is the value of H_0 , used to generate the coefficients in Table 2. An incorrect value of H_0 will directly cause an offset that will change the intercept value and introduce a nonlinearity, which has the potential to change the fit gradient. A plot of $(H_s - H_0)^2$ vs. $1/h$ for the single crystal sample is given in Figure 6, where it can be seen that there is a statistically significant deviation from linearity at large penetration depths. Changing the value of H_0 to 0.75 GPa corrects this non-linearity (see subfigure in Figure 6) and slightly affects the values of k_1 but depresses the value of $k_3\sqrt{\rho_s}$ to be unphysically negative. The sensitivity of these values to H_0 is shown in Table 3. If only the values of k_1 are changed when determining k_2 , this increases LSE k_2 rather than decreasing it. The only other change that would affect the linearity of Figure 6, is to change the exponent of the $(H_s - H_0)^m$ term. If the simplifying assumption is made that $k_3\sqrt{\rho_s}$ is zero for the single crystal data and H_0 remains as 0.045 GPa, a plot of $\log(H_s - H_0)$ vs. $\log 1/h$ gives a value for m of 1.8, which is close to $m=2$. Clearly the linearity of the plot of $(H_s - H_0)^2$ vs. $1/h$ is very sensitive to a small change in the exponent. Unfortunately a value of k_1 obtained from the intercept of the log-log plot is not likely to be valid given that $k_3\sqrt{\rho_s}$ is almost certainly *not* zero. It appears that even the largest physically reasonable errors in H_0 and k_1 are insufficient to explain the large difference between LSE and ISE k_2 . This leaves only the explanation that the effective grain size, when scratching, is four times smaller than the effective grain size when indenting and that scratch testing is much more sensitive to grain size than indentation. This has significant design implications for anti-wear coatings and other tribological interactions. Further research is being conducted to investigate this difference.

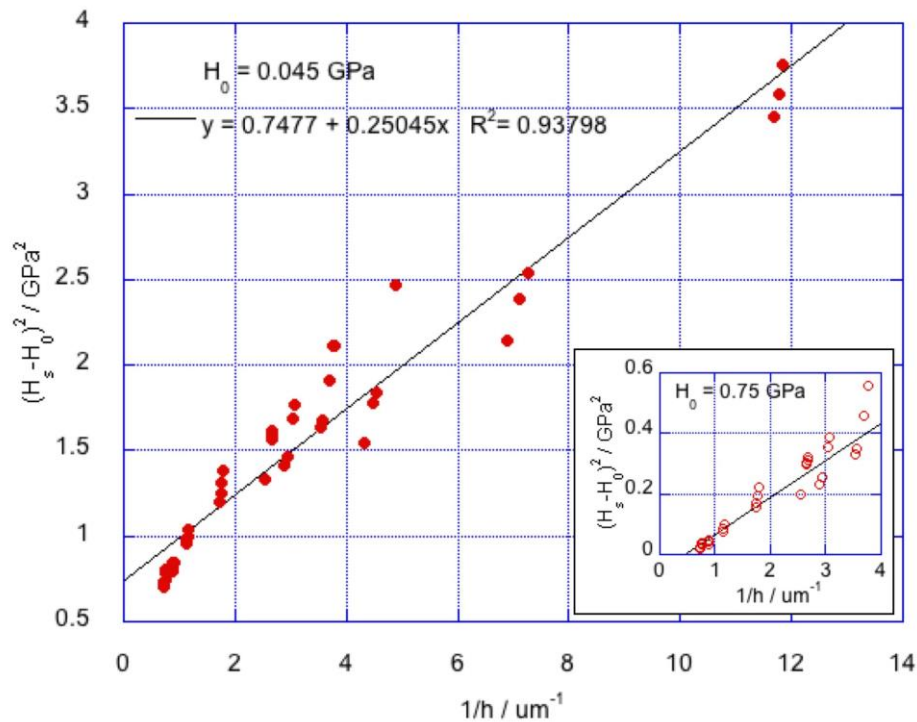


Figure 6 - Plot of $(H_s - H_0)^2$ vs. $1/h$ for the single crystal sample and associated linear least squares fit, where H_0 is taken as 0.045 GPa, subfigure shows plot of $(H_s - H_0)^2$ vs. $1/h$ at large penetration depths, when H_0 is taken as 0.75 GPa.

Table 3 - Effect on k_1 and $k_3\nu\rho_s$ of assuming different infinite length scale hardness values

H_0 / GPa	k_1 for $d=1.2 \mu\text{m}$ /m.GPa ²	k_1 for Single Crystal /m.GPa ²	$k_3\nu\rho_s$ for $d=1.2 \mu\text{m}$ /m.GPa ²	$k_3\nu\rho_s$ for Single Crystal /m.GPa ²
0	0.16	0.25	1.77	0.83
0.045	0.16	0.25	1.57	0.75
0.45	0.13	0.18	0.04	0.17
0.75	0.11	0.12	-0.92	-0.05

It can be seen in Figure 4 that Equation 2 is a good fit to the scratch data, however, the fit at large depths could be better and a reduction in curvature would improve the fit to data in the depth range 200nm - 600nm. Currently the fit asymptotes to a constant value where the combination of grain size and dislocation spacing are dominantly small, whereas the data display a continuing LSE. Equation 2 assumes that $k_3\nu\rho_s$ is constant, but a better fit to the data would be obtained if $k_3\nu\rho_s$ was not constant but decreased with scratch depth. It is quite likely that this happens if the dislocation density experienced by the contact is dominated by the dislocations generated by the act of making the contact itself. In particular, the geometrically necessary dislocation (GND) density required to form the indentation shape in the surface,

decreases with increasing indentation or scratch penetration depth, which would allow the reduction in $k_3\sqrt{\rho_s}$ that is necessary to improve the fit. It should be noted that an ‘across the board’ reduction in $k_3\sqrt{\rho_s}$ acts to increase the curvature of the fit and so only a progressive reduction with scratch depth can help.

The most direct method to reduce fit curvature is to reduce k_I . It is interesting to note from Table 2 that there is a significant interaction between grain size and both k_I and $k_3\sqrt{\rho_s}$: k_I increases with grain size, whereas $k_3\sqrt{\rho_s}$ decreases. [The alternative explanation that k_I increases as $k_3\sqrt{\rho_s}$ decreases is considered causally unlikely, as this would suggest that the critical length associated with plastic zone size decreases as the dislocation density decreases, which is opposite to experience and expectations for work-hardening]. The GND argument above would result in an additional (albeit longer range) contribution to the curvature from the depth dependence of the $k_3\sqrt{\rho_s}$ term, which would suggest that the k_I values might be lower than the current analysis suggests.

In the current analysis, the plastic zone size represented by a/k_I is considered to be an input value. However, it may be that the a/k_I value should be (at least partly) considered as an output value, i.e. the actual plastic zone size achieved in an indentation/scratch is the result of dislocation motion and generation being constrained by obstacles such as grain boundaries and existing dislocation density. It is clear from [18] and from [23] that the effective dislocation density, at any particular scratch or indentation size, is strongly affected by the plastic strain induced by the scratch or indentation. In indentation hardness testing, there has been much attention on using the concept of geometrically necessary dislocations (GNDs) for understanding the deformation beneath indentations (see [13] and [27]). Sarabadi et al [27] used polishing, etching and imaging to reveal the dislocation structures around indentations in CaF₂ single crystal. However, the same plasticity size effects occur in uniaxial deformations where there are no strain gradients driving a geometrically necessary increase in dislocation density. In contrast, the slip-distance-based analysis includes all obstacle spacing’s (including those due to dislocations). The key modification is that it is not the spacing between dislocations per se that counts, but rather the mean free path between those dislocations that provide an obstacle to dislocation motion. To know this by direct characterisation is, in practise, impossible, since the position and nature of all dislocations would have to be known along with the position and nature and direction of motion of all mobile dislocations. Even for small indentations.....

More research is required to investigate the generation of dislocation density as a function of; plastic strain introduced by a scratch or indentation, and strain distribution due to different

stylus geometries. Also required are better measurements of the actual plastic zone sizes generated in these instances.

5. Conclusions

Scratch tests performed on polycrystalline copper have enhanced hardness with reduction of grain size of the material, exhibiting a grain size effect in addition to the lateral size effect previously observed [23] when scratching single crystal copper with different scratch sizes. It has been shown that the increase in scratch hardness is linearly proportional to the inverse square root of the grain size, illustrating a Hall-Petch-like relationship. When the grain size is small, the lateral size effect (i.e. scratch hardness variation as a function of scratch size) is smaller than for a large-grained material or a single crystal. This is a clear indication that the two length-scales combine rather than superpose and that it is the combined length-scale that is responsible for the variation in scratch hardness that has been observed; comparable to that observed in indentation.

Application of slip distance theory generates good fits to the scratch data, which suggests that the lateral size effects (LSE) observed in scratch deformation have strong similarities to the indentation size effects (ISE) observed in indentation. However, there are some interesting differences, in that the absolute values of the fitting parameters obtained in each case are different, despite the scratch and indentation data being obtained from exactly the same samples. Correcting for the use of different proxy parameters (indentation contact size vs. average penetration depth) and allowing for pile up, bring the k_I scaling parameter for scratch and indentation into near agreement. It is then notable that, if scratch deformation is considered as a sideways indentation with the characteristic length-scale being the scratch width, then the k_I scaling parameters for both scratch and indentation are in very close agreement.

In the fit, the scratch hardness begins to plateau at large scratch sizes, however, the measured scratch hardness continues to decrease further. We suggest that a better fit would require a non-constant $k_3\sqrt{\rho_s}$ term, which decreases with increasing penetration depth to account for the continued lateral size effect at large penetration depths. This would suggest that there is a size dependent dislocation generation beneath the scratch, which is not unlikely (for example if GNDs dominate the dislocation density length-scale). In order to understand this fully, quantification of the dislocation density within the plastic zone beneath the scratch would be required.

The most significant difference between LSE and ISE fit parameter values is that the ratio of k_2 values for LSE and ISE differ by over a factor of four. Even the largest physically reasonable

changes to the only input parameters, H_0 and k_I , are insufficient to explain the large difference. This leaves only the explanation that the effective grain size, when scratching, is four times smaller than the effective grain size when indenting. The implication for anti-wear coatings and other tribological interactions is that the sensitivity of scratch hardness to grain size can be four times the sensitivity of indentation hardness to grain size. Further work is required to confirm and investigate this remarkable finding; in particular, more research is needed to investigate how the scratch test interacts with grain boundaries, and whether this interaction could potentially explain the differences between the two tests.

Funding

This project has received funding from the EMPIR programme co-financed by the Participating States and from the European Union's Horizon 2020 research and innovation programme

Appendix

Resolved force calculation for the EF tip orientation. F_r is the resolved force; F_L is the averaged lateral force along steady-state region; F_N is the average normal force along steady state region. The indenter geometry is given in Figure 7. For the EF tip orientation:

$$\frac{1}{2} F_r = \frac{1}{2} F_L \cos \theta \cos 60^\circ + \frac{1}{2} F_N \sin 60^\circ$$

$$F_r = \frac{1}{2} F_L \cos \theta + F_N \sin 60^\circ$$

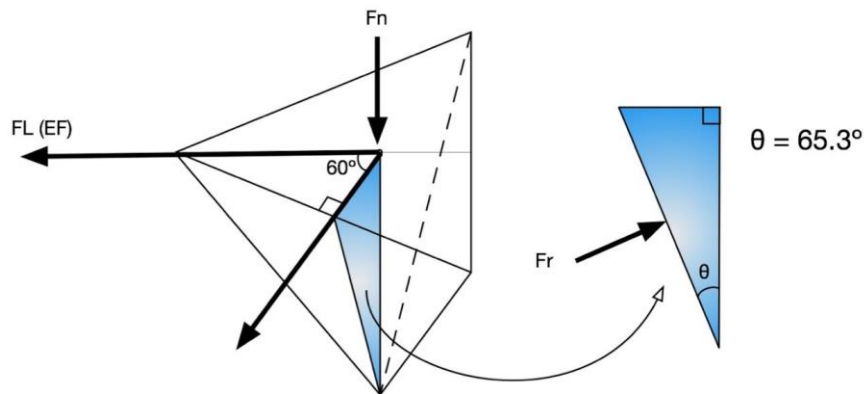


Figure 7 – Geometry of the indenter showing the facets on which the force is resolved for the EF tip orientation.

References

- [1] S. R. Bakshi, D. Lahiri, R. R. Patel, and A. Agarwal, "Nanoscratch behavior of carbon nanotube reinforced aluminum coatings," *Thin Solid Films*, vol. 518, pp. 1703–1711, 2010.

- [2] J.-C. Huang, C.-L. Li, and J.-W. Lee, "The study of nanoscratch and nanomachining on hard multilayer thin films using atomic force microscope," *Scanning*, vol. 34, no. 1, pp. 51–59, 2012.
- [3] K. H. T. Raman, M. S. R. N. Kiran, U. Ramamurty, and G. M. Rao, "Structure and mechanical properties of TiC films deposited using combination of pulsed DC and normal DC magnetron co-sputtering," *Appl. Surf. Sci.*, vol. 258, pp. 8629–8635, 2012.
- [4] E.P. Koumoulos, C. A. Charitidis, D. P. Papageorgiou, A. G. Papathanasiou, and A. G. Boudouvis, "Nanomechanical and nanotribological properties of hydrophobic fluorocarbon dielectric coating on tetraethoxysilane for electrowetting applications," *Surf. Coatings Technol.*, vol. 206, pp. 3823–3831, 2012.
- [5] S. J. Bull, "Failure mode maps in the thin film scratch adhesion test," *Tribology International*, vol. 30, pp. 491–498, 1997.
- [6] S. V Hainsworth, S. J. Bull, and T. F. Page, "Scratch Deformation Response of Thin CN_x Coatings at Ultra-Low Loads," *MRS Online Proc. Libr.*, vol. 522, p. 433–438, 1998.
- [7] S. M. Noh, J. W. Lee, J. H. Nam, J. M. Park, and H. W. Jung, "Analysis of scratch characteristics of automotive clearcoats containing silane modified blocked isocyanates via carwash and nano-scratch tests," *Prog. Org. Coatings*, vol. 74, no. 1, pp. 192–203, 2012.
- [8] J. Xia, C. X. Li, H. Dong, and T. Bell, "Nanoindentation and nanoscratch properties of a thermal oxidation treated γ -TiAl based alloy," *Surf. Coatings Technol.*, vol. 200, pp. 4755–4762, 2006.
- [9] J. Moghal, A. Bird, A. H. Harris, B. D. Beake, M. Gardener, and G. Wakefield, "Nanomechanical study of thin film nanocomposite and PVD thin films on polymer substrates for optical applications," *J. Phys. D. Appl. Phys.*, vol. 46, no. 48, p. 485303, 2013.
- [10] N. Tayebi, T. F. Conry, and A. A. Polycarpou, "Reconciliation of nanoscratch hardness with nanoindentation hardness including the effects of interface shear stress," *J. Mater. Res.*, vol. 19, no. 11, pp. 3316–3323, 2004.
- [11] J. A. Williams, "Analytical models of scratch hardness," *Tribol. Int.*, vol. 29, pp. 675–694, 1996.
- [12] I. J. Spary, A. J. Bushby, and N. M. Jennett, "On the indentation size effect in spherical indentation," *Philoso. Mag.* vol. 86. pp. 5581–5593, 2006.
- [13] W. D. Nix and H. Gao, "Indentation size effects in crystalline materials: A law for strain gradient plasticity," *Journal of the Mechanics and Physics of Solids*, vol. 46. pp. 411–425, 1998
- [14] Y. Yee Lim, M. M. Chaudhri, "The effect of the indenter load on the nanohardness of ductile metals: an experimental study on polycrystalline work-hardened and annealed oxygen-free copper," *Philosophical Magazine A*, vol. 79. pp. 2979–3000, 1999.
- [15] E. O. Hall, "The Deformation and Ageing of Mild Steel: III Discussion of Results," *Proc. Phys. Soc. Sect. B*, vol. 64, no. 9, p. 747, 1951.
- [16] N. J. Petch, "The influence of grain boundary carbide and grain size on the cleavage strength and impact transition temperature of steel," *Acta Metall.*, vol. 34, no. 7, pp. 1387–1393, Jul. 1986.
- [17] X. D. Hou, A. J. Bushby, and N. M. Jennett, "Study of the interaction between the indentation size effect and Hall–Petch effect with spherical indenters on annealed polycrystalline copper," *J. Phys. D. Appl. Phys.*, vol. 41, no. 7, p. 074006, 2008.
- [18] X. D. Hou and N. M. Jennett, "Application of a modified slip-distance theory to the indentation of single-crystal and polycrystalline copper to model the interactions between indentation size and structure size effects," *Acta Mater.*, vol. 60, pp. 4128–4135, 2012
- [19] Taylor, G. I. (1938). Plastic Strain in Metals. *Journal of the Institute of Metals*, 62:307–324.

- [20] J. Swadener, “The correlation of the indentation size effect measured with indenters of various shapes,” *Journal of the Mechanics and Physics of Solids*, vol. 50, pp. 681–694, 2002.
- [21] 1795-1871 Mohs, F. 1773-1839 Haidinger, Wilhelm, *Treatise on mineralogy, or, The natural history of the mineral kingdom*, Vol. 1. Edinburgh: Printed for A. Constable, 1825.
- [22] ASTM, “ASTM G171 Standard Test Method for Scratch Hardness of Materials Using a Diamond Stylus,” *ASTM Stand.*, vol. 03, 2009.
- [23] A. Kareer, X. D. Hou, N. M. Jennett and S. V. Hainsworth “The existence of a lateral size effect and the relationship between indentation and scratch hardness” *Philos. Mag.* published online 24 March 2016, <http://dx.doi.org/10.1080/14786435.2016.1146828>.
- [24] D. G. Flom and R. Komanduri, “Some indentation and sliding experiments on single crystal and polycrystalline materials,” *Wear*, vol. 252, no. 5–6, pp. 401–429, 2002.